Journal of Power Sources 185 (2008) 473–479

Contents lists available at ScienceDirect

Journal of Power Sources

journal homepage: www.elsevier.com/locate/jpowsour

Surface modification of $LiNi_{1/2}Mn_{3/2}O_4$ thin-films by zirconium alkoxide/PMMA composites and their effects on electrochemical properties

Takayuki Doi[a,*], Jun-ichi Kageura[b], Shigeto Okada[a], Jun-ichi Yamaki[a]

[a] Institute for Materials Chemistry and Engineering, Kyushu University, 6-1 Kasuga-koen, Kasuga 816-8580, Japan
[b] Interdisciplinary Graduate School of Engineering Sciences, Kyushu University, 6-1 Kasuga-koen, Kasuga 816-8580, Japan

ARTICLE INFO

Article history:
Received 4 June 2008
Received in revised form 9 July 2008
Accepted 10 July 2008
Available online 17 July 2008

Keywords:
Lithium-ion battery
Surface modification
$LiNi_{1/2}Mn_{3/2}O_4$
Spinel
High-potential positive electrode

ABSTRACT

Three kinds of surface modifications were carried out on $LiNi_{1/2}Mn_{3/2}O_4$ thin-films to improve the charge and discharge characteristics of $LiNi_{1/2}Mn_{3/2}O_4$ positive electrodes. Among them, $Zr(OBu)_4$/poly(methyl methacrylate) (PMMA)-treated $LiNi_{1/2}Mn_{3/2}O_4$ thin-film electrodes showed charge and discharge efficiency of 80–84% in the first cycle, which was much higher than that for an untreated $LiNi_{1/2}Mn_{3/2}O_4$ thin-film electrode (73%). The values of the charge and discharge efficiency were still higher than that for an untreated electrode after the 30th cycle. The charge and discharge curves gave two plateaus at around 4.72 and 4.76 V, which were very similar to those for the untreated electrode. Ac impedance spectroscopy revealed that the surface film resistance should not increase by $Zr(OBu)_4$/PMMA treatment. XPS measurements suggest that a composite layer should be formed on a $LiNi_{1/2}Mn_{3/2}O_4$ thin-film electrode from PMMA and $Zr(OBu)_4$-derived compounds introducing an electrolyte. This composite layer was lithium-ion conductive, and was sustainable enough to suppress subsequent decomposition of an electrolyte at potentials as high as 4.7 V.

1. Introduction

Rechargeable lithium-ion batteries have found widespread use in a variety of electronic devices. However, since the power consumption of electronic devices has increased due to their enhanced performance, the power and energy densities of lithium-ion batteries need to be improved still further. Commercially available lithium-ion batteries generally use lithium 3d-transition metal oxides such as $LiCoO_2$ as a positive electrode material. $LiCoO_2$ works at around 3.9 V and shows an acceptably large capacity of around 140 mAh g^{-1}. The energy density of lithium-ion batteries can increase by using positive electrode materials with large capacities and/or high working potentials. Several kinds of active materials with working potentials higher than that of $LiCoO_2$ have been reported [1–3]. Among them, $LiNi_{1/2}Mn_{3/2}O_4$ exhibits extremely positive potentials at around 4.7 V compared to $LiCoO_2$ [3]. However, at such high potentials, most conventional electrolyte solutions should be thermodynamically unstable. In fact, considerable experimental evidence supports the notion that electrolytes are oxidatively decomposed [4–5]. Irreversible decomposition of electrolytes lowers the coulombic efficiency.

One of the practical approaches to suppress the electrolyte decomposition is the formation of a protective layer on the $LiNi_{1/2}Mn_{3/2}O_4$ electrode surface. The protective layer should be conductive for lithium ions, but electronically insulating so that the electrochemical lithium-ion insertion and extraction reactions at $LiNi_{1/2}Mn_{3/2}O_4$ can proceed even after prolonged charge and discharge cycles. Several kinds of solid polymer electrolytes, which consist of a solid polymer and a lithium salt, have been known to be tolerant at high electrode potentials over 4 V [6]. In addition, in contrast to inorganic ceramic electrolytes, polymer electrolytes conform to the volume changes of the electrodes that typically occur during the charge and discharge reactions; the interfacial connection between the electrode and electrolyte should remain unchanged after repetitive cycles. Hence, a thin polymer-electrolyte seems to be suitable as a protective layer on high-potential positive electrodes. However, the lithium-ion conductivity in a polymer electrolyte is not so high when compared to that in a liquid electrolyte. Rapid lithium-ion transport through a protective layer is essential for suppressing overpotential, in particular, during charging. Several types of composite electrolytes, which consist of polymers and ceramic particles, were reported to exhibit high lithium-ion conductivity due to the lithium-ion conduction in an interfacial region between the polymers and ceramic grains [7].

In the present work, three kinds of surface modifications on $LiNi_{1/2}Mn_{3/2}O_4$, such as coating with a $Zr(OBu)_4$/poly(methyl methacrylate) (PMMA) mixture followed by heating at a temper-

* Corresponding author. Tel.: +81 92 583 7657; fax: +81 92 583 7791.
E-mail address: doi@cm.kyushu-u.ac.jp (T. Doi).

0378-7753/$ – see front matter © 2008 Elsevier B.V. All rights reserved.
doi:10.1016/j.jpowsour.2008.07.013

ature as low as 423 K, were investigated to improve the charge and discharge characteristics of $LiNi_{1/2}Mn_{3/2}O_4$ electrodes. Thin films of $LiNi_{1/2}Mn_{3/2}O_4$ were used here as test electrodes. The electrode surface reactions can be emphasized by using thin films compared to micrometer-sized powders, since the majority of the $LiNi_{1/2}Mn_{3/2}O_4$ grains were exposed to the surface of the thin films to organize into an interface with an electrolyte solution [8].

2. Experimental

A $LiNi_{1/2}Mn_{3/2}O_4$ thin-film was prepared on a Pt substrate by the sol–gel method. Lithium acetate dihydrate ($CH_3COOLi{\cdot}2H_2O$, Kanto Chemicals), manganese acetate tetrahydrate ($Mn(CH_3COO)_2{\cdot}4H_2O$, Wako Pure Chemical Industries), and nickel acetate tetrahydrate ($Ni(CH_3COO)_2{\cdot}4H_2O$, Wako Pure Chemical Industries) were used as lithium, manganese, and nickel sources, respectively. These were dissolved in ethanol containing 2-ethylhexanoic acid (Nakalai Tesque) and polyvinylpyrrolidone K-90 (Nakalai Tesque). The precursor solution was spin-coated on a Pt substrate at 3000 rpm for 20 s, and then dried to obtain a precursor film. The precursor film was heated at various temperatures ranging from 773 to 1073 K for 1 h in air using an electric furnace to obtain a $LiNi_{1/2}Mn_{3/2}O_4$ thin-film. X-ray diffraction (XRD) patterns of the thin films were obtained using a Rint-2100 (Rigaku) equipped with a graphite monochromator with a scintillation detector. Typical working conditions were 50 kV and 300 mA with a scanning speed of $0.1^\circ\,min^{-1}$. Raman spectra were excited using the 514.5 nm line (100 mW) of an argon ion laser, and the scattered light collected in a quasi-backscattering geometry. All spectra were recorded using a spectrometer (NRS-2100, Jasco) equipped with a multichannel charge coupled device detector. Each measurement was carried out at room temperature with an integration time of 60 s. Fractured cross-sections of the resultant films deposited on a Si substrate were observed by scanning electron microscopy (SEM) (JSM-6340F, JEOL) to evaluate the thickness.

Three kinds of coating solutions were used. The first was a mixture of SiO_2 particles (Aldrich) and PMMA (degree of polymerization = 7000, Nakalai Tesque) dissolved in acetone (Wako Pure Chemical Industries). The concentration of SiO_2 and PMMA in the solution was 1.5 and 1.0 wt%, respectively. This coating solution was spin-coated onto $LiNi_{1/2}Mn_{3/2}O_4$ thin-films at 1000 rpm for 15 s, and then heated at 373 K for 6 h. Another solution was prepared from zirconium *n*-butoxide ($Zr(OC_4H_9)_4$, Mitsuwa Chemicals) and *n*-butanol (Wako Pure Chemical Industries). The concentration of $Zr(OC_4H_9)_4$ in solution was equivalent to 0.66 wt% ZrO_2. The other solution was a mixture of $Zr(OC_4H_9)_4$ and PMMA (0.14 wt%) in acetone, where the concentration of $Zr(OC_4H_9)_4$ in solution was equivalent to 0.66 wt% ZrO_2. The latter two solutions were spin-coated onto $LiNi_{1/2}Mn_{3/2}O_4$ thin-films at 1000 rpm for 20 s, and then heated at 423 K for 1 h.

The electrochemical properties of surface-treated $LiNi_{1/2}Mn_{3/2}O_4$ thin-films were measured using a three-electrode cell. The effective electrode surface area was limited to 0.47 cm^2 by an o-ring. Both the counter and reference electrodes used were lithium metal. The electrolyte solution was $LiPF_6$ dissolved in a mixture of ethylene carbonate (EC) and dimethyl carbonate (DMC) (1:1 v/v, Tomiyama Pure Chemical Industries). Charge and discharge tests (HJ1001SM8A, Hokuto Denko) and cyclic voltammetry (Parstat 2263, Princeton Applied Research) were carried out between 4.4 and 4.9 V at a constant current of 1 $\mu A\,cm^{-2}$ and at a scan rate of 0.05 $mV\,s^{-1}$, respectively. After charge and discharge measurements, the electrolyte solution was removed from the cell and the working electrode was rinsed with DMC. The active materials of the working electrode (surrounded by an o-ring) were then dissolved in hydrochloric acid (Nakalai Tesque). The amount of active materials was evaluated from this solution by atomic absorption spectrophotometry (Z-5310, Hitachi). Lithium-ion transport within the interfacial region between the electrode and electrolyte was investigated by ac impedance spectroscopy using a Parstat 2263. Before potential cycling and after the 10th cycle between 4.4 and 4.9 V, the working electrode was kept at 3.5 V to reach a steady state. Ac impedance spectra were then obtained by applying a sine wave with an amplitude of 10 mV over a frequency range from 1 MHz to 10 mHz. Unless otherwise stated, the potential is given vs. Li/Li^+. All experiments were conducted at 25 °C under an argon atmosphere with a dew point below −70 °C.

The surface of the $LiNi_{1/2}Mn_{3/2}O_4$ thin-film electrodes was investigated by X-ray photoelectron spectroscopy (XPS, JPS-9010MC/IV, JEOL) with monochromatic Mg Kα radiation (1253.6 eV). After the charge and discharge cycles, the cells were disassembled in an Ar-filled glove box. The test electrode was rinsed and soaked with DMC for 4 h, and then was dried under vacuum in the glove box at room temperature to remove low-molecular weight compounds. It was sealed in a vessel under an argon atmosphere to transfer into a sample chamber of an XPS instrument without being exposed to air. C1s spectra were obtained by repeated scans using a pass-energy of 10 eV to calibrate the peak positions by reference to the C1s level of 285.0 eV.

3. Results and discussion

Fig. 1 shows XRD patterns of the resultant films obtained at 773, 873, 973, and 1073 K. The pattern indicates that a single-phase spinel $LiNi_{1/2}Mn_{3/2}O_4$ was obtained at temperatures from 773 to 1073 K. The peaks of 2θ angles at 18.7°, 36.4°, 38.1°, 44.3°, 48.4°, 58.7°, and 64.4° corresponded to the (1 1 1), (3 1 1), (2 2 2), (4 0 0), (3 3 1), (5 1 1), and (4 4 0) diffraction lines, respectively [3]. The peaks at 39.9°, 46.3°, and 67.6° were assigned to the diffraction lines of Pt. The full width at half maximum (FWHM) of (4 4 0) diffraction lines was evaluated to be 0.66°, 0.65°, 0.43,° and 0.42° for the $LiNi_{1/2}Mn_{3/2}O_4$ thin-films prepared at 773, 873, 973, and 1073 K, respectively. Thus, the values of FWHM showed little change at temperatures above 973 K. These results indicate that the $LiNi_{1/2}Mn_{3/2}O_4$ thin-film heated at 973 K was highly crystallized. Hence, the $LiNi_{1/2}Mn_{3/2}O_4$ thin-films prepared at 973 K were used in this study hereafter. ICP-MS measurements revealed that

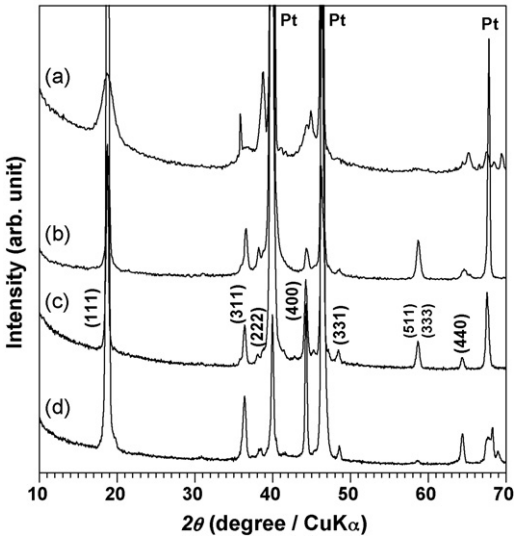

Fig. 1. XRD patterns of Li–Ni–Mn–O thin-films prepared at (a) 773, (b) 873, (c) 973, and (d) 1073 K.

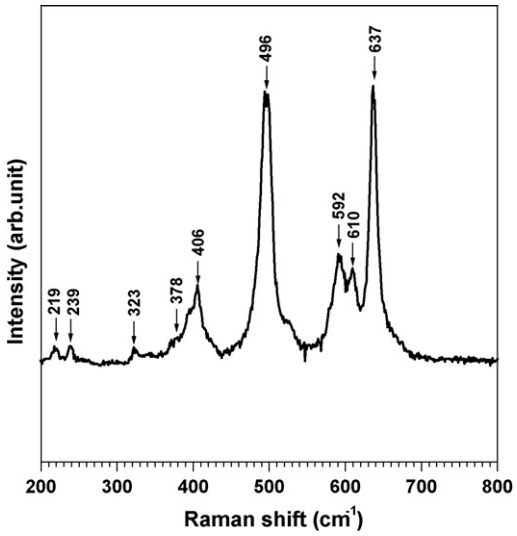

Fig. 2. Raman spectrum of a $LiNi_{0.5}Mn_{1.5}O_4$ thin-film prepared at 973 K.

the Li/Ni/Mn atomic ratio of the film was 1.06/0.484/1.50. Therefore, nearly stoichiometric spinel $LiNi_{0.5}Mn_{1.5}O_4$ thin-films were obtained in this work.

Fig. 2 shows the Raman spectrum of a $LiNi_{1/2}Mn_{3/2}O_4$ thin-film prepared at 973 K. Five main peaks appeared around 406, 496, 592, 610 and 637 cm^{-1}. Moreover, three small peaks were also observed at 219, 239, and 323 cm^{-1}. Although the assignment of each signal has not yet been clarified, this spectrum is in good agreement with that reported in the literature [9]. Therefore, the resultant $LiNi_{1/2}Mn_{3/2}O_4$ thin-film has a spinel framework structure having a space group of $P4_332$.

Fig. 3a shows cyclic voltammograms of a $LiNi_{1/2}Mn_{3/2}O_4$ thin-film between 4.4 and 5.0 V. Two couples of redox peaks were observed at around 4.72 and 4.75 V, which are characteristic of $LiNi_{1/2}Mn_{3/2}O_4$, except in the first cycle. In the initial anodic scan, the peak potentials were very high and the peak shapes were broad, while the corresponding cathodic peak was quite similar to those after the second cycle. At such positive potentials of around 4.7 V, most conventional electrolyte solutions should be thermodynamically unstable. In fact, considerable experimental evidence supports the notion that electrolytes are oxidatively decomposed to form a passivating surface film on the electrode, particularly during the initial charging [4–5]. Hence, the anomalous behavior during the initial anodic scan is likely due to the electrolyte decomposition. After the second cycle, the peak separation in potential was as small as 11 mV for both couples at ca. 4.72 and 4.75 V.

The charge and discharge measurements of a $LiNi_{1/2}Mn_{3/2}O_4$ thin-film were carried out to discuss the reversibility of the electrode reactions quantitatively. Charge and discharge curves are shown in Fig. 3b. Two plateaus appeared at around 4.72 and 4.76 V during charge and discharge cycles, which corresponded to the two couples of redox peaks in the cyclic voltammograms shown in Fig. 3a. The discharge capacity in the first cycle was 129 mAh g^{-1} since the amount of active materials was evaluated to be 7.79 μg by atomic absorption spectrophotometry. The charge and discharge efficiency, which signifies the proportion of discharge capacity to charge capacity in a charge and discharge cycle, was as low as about 73% in the first cycle, while above 86% after the second cycle. The irreversible capacity in the first cycle was 35 mAh g^{-1}, which is larger than those for the micrometer-sized $LiNi_{1/2}Mn_{3/2}O_4$ particles reported in the literature [10]. The thickness of the $LiNi_{1/2}Mn_{3/2}O_4$ thin-film was estimated to be about 0.2 μm from the SEM images. The original grain size of $LiNi_{1/2}Mn_{3/2}O_4$ was

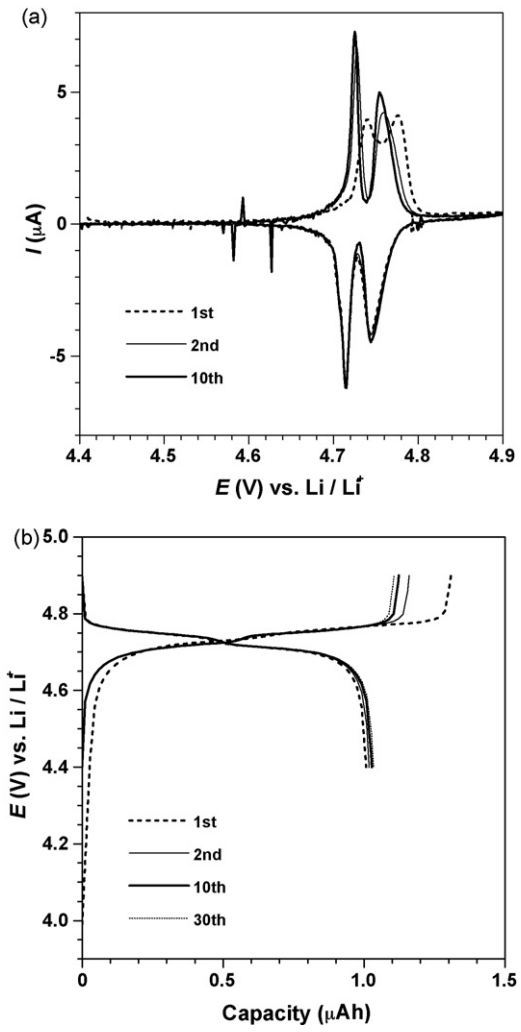

Fig. 3. (a) Cyclic voltammograms and (b) charge and discharge curves of $LiNi_{0.5}Mn_{1.5}O_4$ thin-films prepared at 973 K.

around 0.1 μm, and hence about a half of the grains would be exposed to the surface of the thin film to organize into an interface with an electrolyte solution. These facts suggest that irreversible reactions should be more serious for the $LiNi_{1/2}Mn_{3/2}O_4$ surface than for its interior; electrolyte decomposition would occur significantly on the $LiNi_{1/2}Mn_{3/2}O_4$ surface. Several organic and inorganic species, including lithium fluoride and lithium alkylcarbonate, were found on the $LiNi_{1/2}Mn_{3/2}O_4$ thin-film electrodes after the 30th cycle by XPS. If a protective film was effectively formed on the $LiNi_{1/2}Mn_{3/2}O_4$ surface so that the further decomposition of the electrolyte can be suppressed, the charge and discharge efficiency of a $LiNi_{1/2}Mn_{3/2}O_4$ thin-film electrode would be improved. In this work, surface modification of a $LiNi_{1/2}Mn_{3/2}O_4$ thin-film was carried out to produce a novel surface film.

A layer consisting of SiO_2 and PMMA was formed on a $LiNi_{1/2}Mn_{3/2}O_4$ thin-film. The SiO_2 particles used here had an average particle size of 10 nm. The charge and discharge curves of the SiO_2/PMMA-treated $LiNi_{1/2}Mn_{3/2}O_4$ thin-film electrode (not shown) were quite similar to those of an untreated $LiNi_{1/2}Mn_{3/2}O_4$ thin-film electrode shown in Fig. 3b. The variation of charge and discharge efficiency with cycle number, which is shown in Fig. 4, was also very similar to those for an untreated electrode; the SiO_2/PMMA-treated $LiNi_{1/2}Mn_{3/2}O_4$ thin-film electrode showed a charge and discharge efficiency as low as 73%, while above 85%

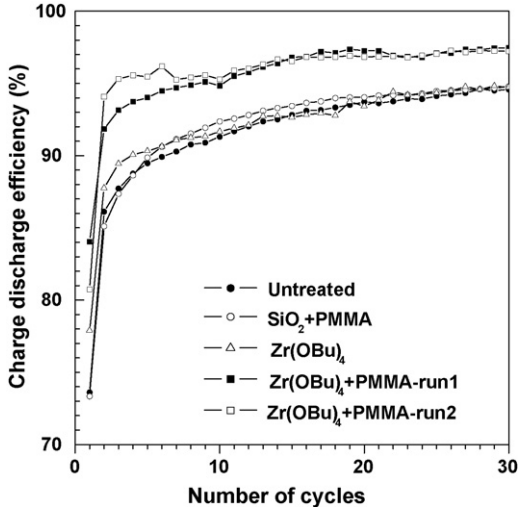

Fig. 4. Charge and discharge efficiency of untreated, SiO_2/PMMA-treated, $Zr(OBu)_4$-treated, and $Zr(OBu)_4$/PMMA-treated $LiNi_{0.5}Mn_{1.5}O_4$ thin-film electrodes.

after the second cycle. XPS measurements revealed that the peaks attributed to PMMA were non-existent in the C1s and O1s spectra after the charge and discharge cycles. In addition, the peaks identified as Ni–O and Mn–O bonds were newly appeared in the O1s spectra after the charge and discharge cycles. These results indicate that a SiO_2/PMMA layer was dissolved into the electrolyte solution, and then the $LiNi_{1/2}Mn_{3/2}O_4$ thin-film barely appeared on the surface. Hence, there was no improvement in the charge and discharge characteristics by SiO_2/PMMA treatment.

Several kinds of inorganic materials such as Al_2O_3, SnO_2 and ZrO_2 were reported as protective surface layers to improve the charge and discharge characteristics of $LiCoO_2$ [11–13]. However, it is difficult to cover particles of active materials with inorganic materials such as ZrO_2 by existing techniques because both materials are solid. In this work, an inorganic layer was formed using a $Zr(OBu)_4$-containing solution on a $LiNi_{1/2}Mn_{3/2}O_4$ thin-film. The charge and discharge curves of the $Zr(OBu)_4$-treated $LiNi_{1/2}Mn_{3/2}O_4$ thin-film electrode are shown in Fig. 5a. These were quite similar to those of the untreated $LiNi_{1/2}Mn_{3/2}O_4$ thin-film electrode shown in Fig. 3b. The initial discharge capacity was 145 mAh g^{-1}, which is larger than that for the untreated electrode. The charge and discharge efficiency in the first cycle increased to

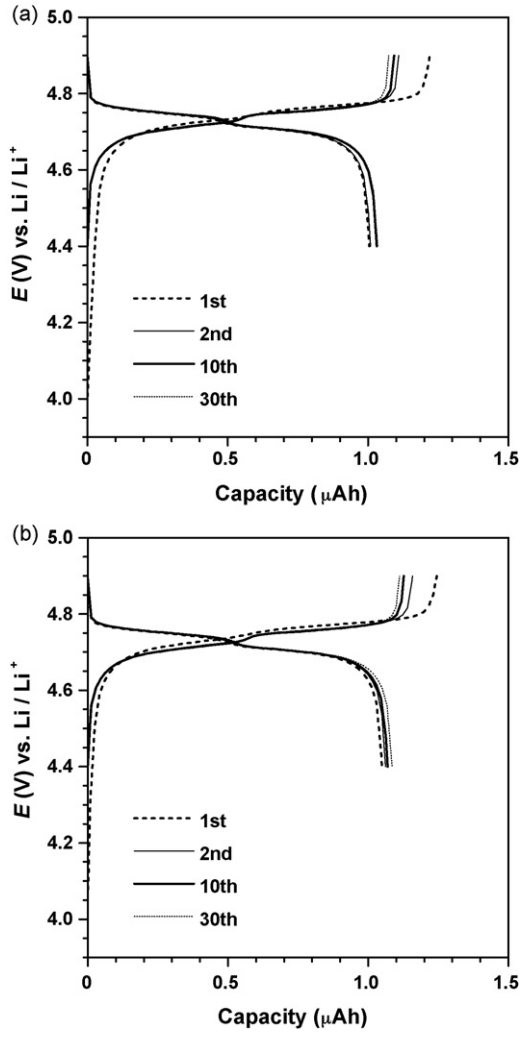

Fig. 5. Charge and discharge curves of (a) $Zr(OBu)_4$-treated and (b) $Zr(OBu)_4$/PMMA-treated $LiNi_{0.5}Mn_{1.5}O_4$ thin-film electrodes.

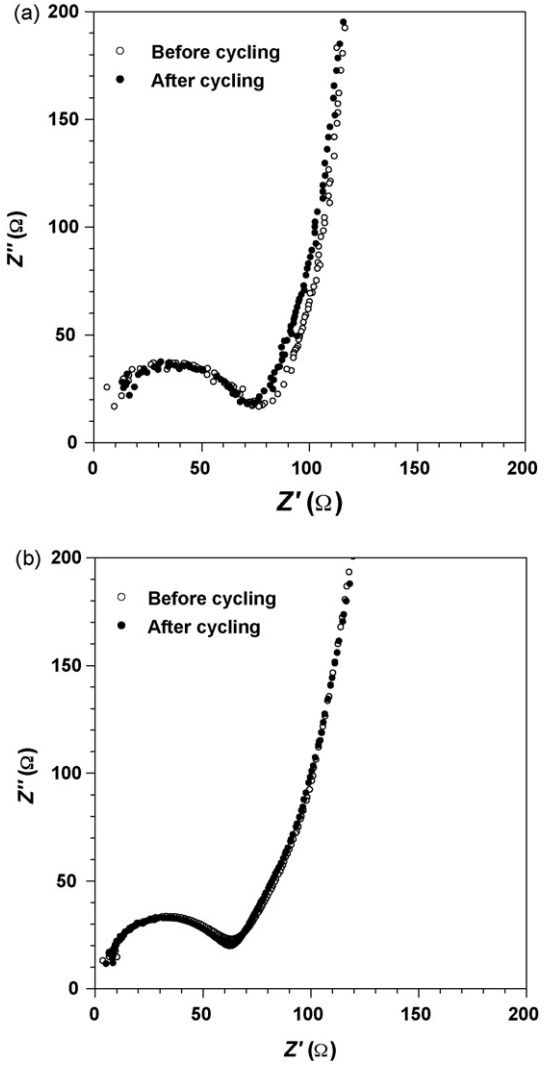

Fig. 6. Impedance spectra of (a) untreated and (b) $Zr(OBu)_4$/PMMA-treated $LiNi_{0.5}Mn_{1.5}O_4$ thin-film electrodes before and after the 30th potential cycling.

78% by $Zr(OBu)_4$ treatment, as shown in Fig. 4. Although the values of the charge and discharge efficiency were larger than those for an untreated electrode, at least until the fifth cycle where they were almost similar to each other after the sixth cycle. The Zr3d spectra of the $Zr(OBu)_4$-treated $LiNi_{1/2}Mn_{3/2}O_4$ thin-films showed peaks at 182.7 and 185.0 eV before immersing them into an electrolyte. These peaks should be assigned to the products afforded by hydrolytic polycondensation of $Zr(OBu)_4$. The surface layer prepared from $Zr(OBu)_4$ would be electrochemically inactive, and hence it shows no lattice expansion and contraction during charge and discharge cycles. On the other hand, Ariyoshi et al. reported that the charge and discharge reactions of $LiNi_{1/2}Mn_{3/2}O_4$ at ca. 4.7 V consisted of two cubic/cubic two-phase reactions; $Ni_{1/2}Mn_{3/2}O_4$ (a = 8.00 Å) was reduced to $LiNi_{1/2}Mn_{3/2}O_4$ (a = 8.17 Å) via $Li_{1/2}Ni_{1/2}Mn_{3/2}O_4$ (a = 8.09 Å) during discharge, and the reverse reactions occurred during charge. The lattice volume varies by 5.9% between $Ni_{1/2}Mn_{3/2}O_4$ and $LiNi_{1/2}Mn_{3/2}O_4$ [3]. Hence, the $Zr(OBu)_4$-derived surface layer would become stressed during the cycles. The surface layer would be cracked and/or removed from the $LiNi_{1/2}Mn_{3/2}O_4$ thin-film surface, and therefore the charge and discharge efficiency of the $Zr(OBu)_4$-treated $LiNi_{1/2}Mn_{3/2}O_4$ thin-film electrode would be degraded to the same values as an untreated electrode after repeated cycles.

A PMMA/$Zr(OBu)_4$ composite formed on a $LiNi_{1/2}Mn_{3/2}O_4$ thin-film should be more flexible than a $Zr(OBu)_4$-derived surface layer as described above. The charge and discharge curves of the $Zr(OBu)_4$/PMMA-treated $LiNi_{0.5}Mn_{1.5}O_4$ thin-film electrode are shown in Fig. 5b. Two plateaus were observed at around 4.72 and 4.76 V during the charge and discharge cycles, respectively. Although the plateaus gave higher potentials by 10 mV than that for an untreated electrode during the initial charging, the electrode potentials were almost the same as those for an untreated electrode after the second cycle. These results suggest that the internal resistance would not increase by $Zr(OBu)_4$/PMMA treatment of a $LiNi_{0.5}Mn_{1.5}O_4$ thin-film. The discharge capacity was 135 mAh g^{-1} in the first cycle. The charge and discharge efficiency increased to 80–84% in the first cycle by $Zr(OBu)_4$/PMMA treatment, and was still higher than that for an untreated electrode after the 30th cycle, as shown in Fig. 4. Both $Zr(OBu)_4$/PMMA-run1 and -run2 in Fig. 4 were obtained by conducting the same experiment repeatedly. These

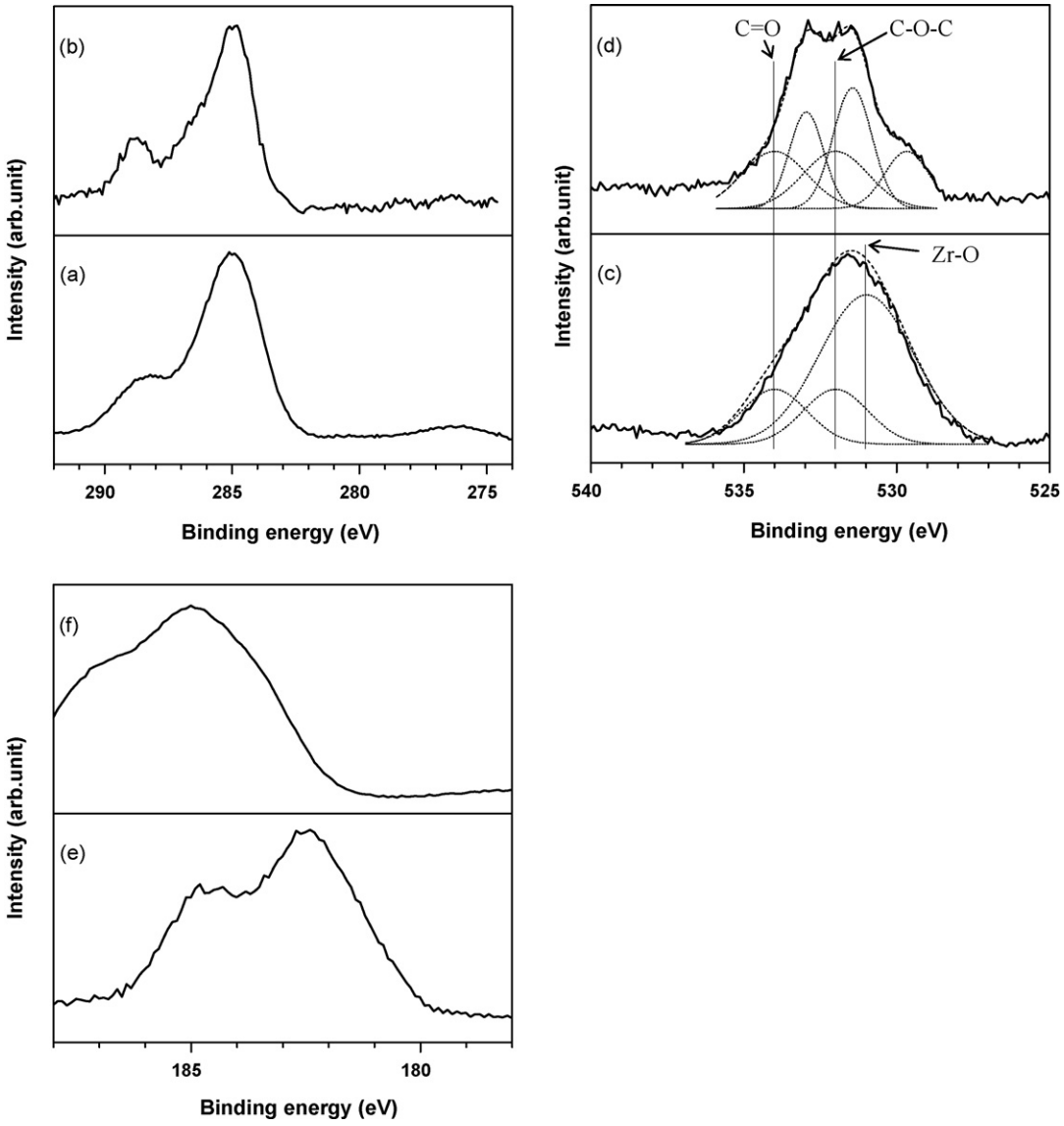

Fig. 7. (a and b) C1s, (c and d) O1s, and (e and f) Zr3d spectra of $Zr(OBu)_4$/PMMA-treated $LiNi_{0.5}Mn_{1.5}O_4$ thin-films. (a, c, and e) and (b, d, and f) were obtained for as-prepared $Zr(OBu)_4$/PMMA-treated thin-films and for those after the 30th cycle, respectively. A broken line shows the fitted curve in which each curve is indicated by a dotted line.

results indicate that the oxidative decomposition of an electrolyte could be suppressed by $Zr(OBu)_4$/PMMA treatment.

Fig. 6 shows Nyquist plots of the $Zr(OBu)_4$/PMMA-treated $LiNi_{0.5}Mn_{1.5}O_4$ thin-film in 1 mol dm^{-3} $LiPF_6$/EC + DMC at 3.5 V, together with those of untreated $LiNi_{0.5}Mn_{1.5}O_4$ thin-film for comparison. Each measurement was conducted at 25 °C. The thickness of the $LiNi_{1/2}Mn_{3/2}O_4$ thin-film was estimated to be about 0.2 μm from SEM images, and hence the electric resistance of the thin films was quite low. A semi-circle was seen in the higher frequency region even before cycling in Fig. 6a. Aurbach and co-workers reported very similar results [14]. They suggested that surface species, such as Li_2CO_3 or LiF, could be immediately formed on a $LiNi_{0.5}Mn_{1.5}O_4$ electrode when the electrode was immersed into electrolyte solution, and hence a semi-circle assigned to surface film resistance appeared even before cycling. The dimension of the semi-circle in the higher frequency region showed no change after the 30th cycle, as shown in Fig. 6a. Therefore, the surface film resistance did not increase after repeated cycling. Nyquist plots of the $Zr(OBu)_4$/PMMA-treated electrode (Fig. 6b) showed quite similar behavior to those for an untreated electrode. The surface film resistance remained unchanged over repeated cycling up to the 30th cycle, and was estimated to be about 60 Ω. This value was very close to that for an untreated electrode (70 Ω). These results suggested that the surface film resistance could not increase by $Zr(OBu)_4$/PMMA treatment, which is in good agreement with the charge and discharge curves shown in Fig. 5.

The surface layer formed by $Zr(OBu)_4$/PMMA treatment contained no lithium ions, and hence it should be lithium-ion insulating intrinsically. However, this was not the case for the $Zr(OBu)_4$/PMMA-treated $LiNi_{0.5}Mn_{1.5}O_4$ thin-film electrode. The surface film resistance did not increase by $Zr(OBu)_4$/PMMA treatment, and therefore the surface film should be conductive for lithium ions. The surface layer formed by $Zr(OBu)_4$/PMMA treatment would be transformed into another lithium-ion conductive layer by introducing lithium ions from an electrolyte. Fig. 7 shows Zr3d, C1s, and O1s spectra of as-prepared $Zr(OBu)_4$/PMMA-treated $LiNi_{0.5}Mn_{1.5}O_4$ thin-films and those after the 30th cycle. As-prepared $Zr(OBu)_4$/PMMA-treated thin-films showed peaks at 182.7 and 185.0 eV in Zr3d spectra, which should be assigned to products by hydrolytic polycondensation of $Zr(OBu)_4$. The peak at 185.0 eV was still observed after the 30th cycle, but disappeared at 182.7 eV. Another shoulder peak appeared at about 187 eV after the 30th cycle. These results indicate that the products formed by hydrolytic polycondensation of $Zr(OBu)_4$ transform into another Zr-containing compound in an electrolyte. The peaks at 288.5, 532, and 534 eV in C1s and O1s spectra could be assigned to PMMA [15]. These peaks were still observed after the 30th cycle, while there were three fitted curves that could not be identified in O1s spectra. This behavior was quite different from that for a SiO_2/PMMA-treated $LiNi_{0.5}Mn_{1.5}O_4$ thin-film electrode; PMMA could not be seen after the 30th cycle on a SiO_2/PMMA-treated electrode, as described above. PMMA can be dissolved in EC + DMC-based electrolyte solution inherently. However, a composite layer would be formed on a $LiNi_{1/2}Mn_{3/2}O_4$ thin-film electrode from PMMA and $Zr(OBu)_4$-derived compounds introducing an electrolyte, and hence the PMMA could not be dissolved in an electrolyte. By considering the changes in the Zr3d spectra before immersing into an electrolyte and after the charge and discharge cycles, a composite layer would be formed introducing an electrolyte solution when a $Zr(OBu)_4$/PMMA-treated $LiNi_{0.5}Mn_{1.5}O_4$ thin-film electrode was immersed into an electrolyte and/or during initial charging. Thus, a $Zr(OBu)_4$/PMMA-derived composite layer was lithium-ion conductive, and was sustainable enough to suppress subsequent decomposition of an electrolyte at potentials as high as 4.7 V.

4. Conclusion

A nearly stoichiometric $LiNi_{1/2}Mn_{3/2}O_4$ thin-film was prepared on a Pt substrate by a sol–gel method. Two plateaus appeared at around 4.72 and 4.76 V in the charge and discharge curves of the $LiNi_{1/2}Mn_{3/2}O_4$ thin-films, which is characteristic of $LiNi_{1/2}Mn_{3/2}O_4$. The discharge capacity in the first cycle was 129 mAh g^{-1}. The charge and discharge efficiency, which signifies the proportion of the discharge capacity to the charge capacity, was as low as about 73% in the first cycle, while above 86% after the second cycle. To improve the charge and discharge characteristics of $LiNi_{1/2}Mn_{3/2}O_4$, surface modifications of $LiNi_{1/2}Mn_{3/2}O_4$ thin-films were carried out.

A SiO_2/PMMA-treated $LiNi_{1/2}Mn_{3/2}O_4$ thin-film electrode showed similar charge and discharge curves, and the variation of charge and discharge efficiency with cycle number was also very similar to those of an untreated $LiNi_{1/2}Mn_{3/2}O_4$ thin-film electrode. XPS measurements revealed that a SiO_2/PMMA layer was dissolved into an electrolyte after charge and discharge cycles, and the $LiNi_{1/2}Mn_{3/2}O_4$ thin-film barely appeared on the surface. A $Zr(OBu)_4$-treated $LiNi_{1/2}Mn_{3/2}O_4$ thin-film electrode showed charge and discharge curves similar to those of an untreated electrode. Although the charge and discharge efficiency in the first cycle increased to 78% by $Zr(OBu)_4$ treatment compared to an untreated electrode, it degraded to the same values as an untreated electrode after the sixth cycle. The $Zr(OBu)_4$-derived layer would be cracked and/or removed from the $LiNi_{1/2}Mn_{3/2}O_4$ thin-film surface due to the non-conformity of the lattice between the $Zr(OBu)_4$-derived surface layer and $LiNi_{1/2}Mn_{3/2}O_4$ during the charge and discharge reactions.

A PMMA/$Zr(OBu)_4$ composite was formed on a $LiNi_{1/2}Mn_{3/2}O_4$ thin-film, which should be more flexible that a $Zr(OBu)_4$-derived layer. The charge and discharge curves were very similar to those for an untreated electrode and the surface film resistance did not increase by $Zr(OBu)_4$/PMMA treatment. The discharge capacity was 135 mAh g^{-1} in the first cycle. The charge and discharge efficiency increased to 80–84% in the first cycle by $Zr(OBu)_4$/PMMA treatment, and was still higher than that for an untreated electrode after the 30th cycle. XPS measurements suggest that PMMA would form a composite layer with $Zr(OBu)_4$-derived compounds in an electrolyte, and hence the PMMA could not be dissolved in an electrolyte. This composite layer was lithium-ion conductive, and could be sustainable enough to suppress subsequent decomposition of an electrolyte at potentials as high as 4.7 V. Thus, the reversibility of lithium-ion insertion/extraction reactions at $LiNi_{1/2}Mn_{3/2}O_4$ could be improved by forming a PMMA/$Zr(OBu)_4$ composite on a $LiNi_{1/2}Mn_{3/2}O_4$ thin-film.

Acknowledgments

The authors wish to thank Hiroki Ago in Institute for Materials Chemistry and Engineering, Kyushu University, for his kind help on the Raman measurements.

References

[1] M.S. Whittingham, Chem. Rev. 104 (2004) 4271–4301.
[2] S. Okada, S. Sawa, M. Egashira, J. Yamaki, M. Tabuchi, H. Kageyama, T. Konishi, A. Yoshino, J. Power Sources 97–98 (2001) 430.
[3] K. Ariyoshi, Y. Iwakoshi, N. Nakayama, T. Ohzuku, J. Electrochem. Soc. 151 (2004) A296.
[4] K. Kanamura, S. Toriyama, S. Shiraishi, M. Ohashi, Z. Takehara, J. Electroanal. Chem. 419 (1996) 77.
[5] A.M. Andersson, D.P. Abraham, R. Haasch, S. MacLaren, J. Liu, K. Amine, J. Electrochem. Soc. 149 (2002) A1358.
[6] J.-M. Tarascon, M. Armand, Nature 414 (2001) 359.
[7] F. Capuano, F. Croce, B. Scrosati, J. Electrochem. Soc. 138 (1991) 1918.

[8] T. Doi, M. Inaba, H. Tsuchiya, S.-K. Jeong, Y. Iriyama, T. Abe, Z. Ogumi, J. Power Sources 180 (2008) 539.
[9] C.M. Julien, F. Gendron, A. Amdouni, M. Massot, Mater. Sci. Eng. B 130 (2006) 41.
[10] J.-H. Kim, S.-T. Myung, C.S. Yoon, I.-H. Oh, Y.-K. Sun, J. Electrochem. Soc. 151 (2004) A1911.
[11] J. Cho, C.S. Kim, S. Yoo, Electrochem. Solid-State Lett. 3 (2000) 362.
[12] J. Cho, Y.J. Kim, J.T. Kim, B. Park, Angew. Chem. Int. Ed. 18 (40) (2001) 3367.
[13] Z. Chen, J.R. Dahn, Electrochim. Acta 49 (2004) 1079.
[14] Y. Talyosef, B. Markovsky, G. Salitra, D. Aurbach, H.-J. Kim, S. Choi, J. Power Sources 146 (2005) 664.
[15] M.K. Abyaneh, D. Paramanik, S. Varma, S.W. Gosavi, S.K. Kulkarni, J. Phys. D: Appl. Phys. 40 (2007) 3771.